CURRENT MICROBIOLOGY Vol. 43 (2001), pp. 355–364
DOI: 10.1007/s002840010316

Current Microbiology
An International Journal

Effect of Accessory Proteins P19 and P20 on Cytolytic Activity of Cyt1Aa from *Bacillus thuringiensis* subsp. *israelensis* in *Escherichia coli*

Robert Manasherob,[1] Arieh Zaritsky,[1,2] Eitan Ben-Dov,[1] Deepak Saxena,[1,2] Ze'ev Barak,[1] Monica Einav[1]

[1]Department of Life Sciences, Ben-Gurion University of the Negev, P.O. Box 653, Be'er-Sheva 84105, Israel
[2]The Research Institute, The College of Judea and Samaria, Ariel 44837, Israel

Received: 5 March 2001 / Accepted: 3 April 2001

Abstract. The gene coding for the accessory protein P19 of *Bacillus thuringiensis* subsp. *israelensis* was expressed in *Escherichia coli* and its product was characterized. To investigate its putative role in δ-endotoxin crystallization as a P20-like polypeptide, each of the two encoding genes, *p20* and *p19*, was cloned for inducible expression coordinatively with *cyt1Aa*. The latter is known to kill its transgenic host. P20 but not P19 stabilized Cyt1Aa and protected the host cells from its lethal effect. Neither GroEL nor GroES, expressed in *trans*, affected Cyt1Aa as did P20. The function of P20 is thus more specific than that of the chaperones, but that of P19 remains enigmatic. The correct sequence of *p19*, confirmed in all five isolates of *B. thuringiensis* subsp. *israelensis*, does not explain the slow electrophoretic mobility of its 179 amino acids product.

Bacillus thuringiensis is a gram-positive soil bacterium that produces during sporulation [27, 36] large amounts of proteins in the form of crystals (δ-endotoxin). The insecticidal crystal proteins (ICPs) are toxic against a wide variety of insect larvae, mostly of Lepidopteran, Coleopteran, and Dipteran species. The ability to accumulate such quantities of these proteins within the cell is mainly due to their precipitation and aggregation, thus rendering them protease-resistant [5]. All subspecies include at least one Cry polypeptide (for crystal) of 65–145 kDa, and some (with anti-Dipteran specific activity) contain in addition a smaller protein, Cyt (for cytotoxic), of 25–28 kDa. The latter are less specific, hemolytic, and cytotoxic in vitro [22, 39], and not homologous to any of the Cry toxins, but may share a similar mechanism involving colloid-osmotic lysis [24, 25].

The C-terminal half of the large ICPs (125–145 kDa) is conserved and participates in crystal formation. These polypeptides spontaneously form biologically active inclusions probably via inter- and intra-molecular disulfide bonds [2, 3, 9, 14, 36]. The smaller ICPs (< 70 kDa), on the other hand, do not possess this conserved domain [22] and may thus require assistance in crystal formation. There is evidence that Cry2Aa (71 kDa) from *B. thuringiensis* subsp. *kurstaki*, and Cry11Aa (72 kDa) and Cyt1Aa (27 kDa) from *B. thuringiensis* subsp. *israelensis*, require the accessory proteins Orf2 and P20, respectively, for crystallization [1, 15, 32, 40, 46]. The apparent similarity in interactions between the Cry2Aa/Orf2 and Cry11Aa/P20 systems is reflected in their gene organization. They are organized in an operon and co-transcribed with another gene not involved in toxicity, *orf1* and *p19*, respectively [5, 17, 43]. The function(s) of the latter is(are) not known.

The presence of P20 seems to raise the levels of Cyt1Aa and Cry11Aa by post-translational stabilization in recombinant *Escherichia coli* [1, 40] and acrystalliferous strains of *B. thuringiensis* [12, 13, 45, 46]. Similarly, disruption of *orf2* leads to dramatic reduction of Cry2Aa and lack of Cry2Aa crystals in its original host *B. thuringiensis* subsp. *kurstaki* [15]. Moreover, expression of cloned *cyt1Aa* is lethal to *E. coli* [19] and *B. thuringiensis* subsp. *kurstaki* (cryB) cells [45]. Loss of colony-forming ability without substantial lysis, associated with immediate inhibition of DNA synthesis, was observed after induction of recombinant *E. coli* cells

Correspondence to: Robert Manasherob; *email:* ariehz@bgumail.bgu.ac.il

[19]. Thus, both Orf2 and P20 may act as chaperones to initiate, facilitate, or stabilize crystal formation in their original hosts, and protect *E. coli* and *B. thuringiensis* strains from the lethal action of Cyt1Aa. The fact that Cyt1Aa is not lethal to the acrystalliferous strain of *B. thuringiensis* subsp. *israelensis* 4Q7 as it is to *B. thuringiensis* subsp. *kurstaki* raised the possibility [45] that another protein with a function similar to that of P20 exists in subsp. *israelensis*. The newly discovered P19, whose encoding gene is mapped upstream of *cry11Aa* and *p20* [17] may be involved in crystallization or stabilization of Cyt1Aa [2, 5, 17]. This hypothesis implies that P19 may also protect *E. coli* cells from the lethal action of Cyt1Aa.

P19 includes over 11% residues of cysteine and resembles Orf1 (with 33% identity) [17]. The latter is encoded by the first gene of the *cry2Aa* operon [43], but has no detectable effect on the synthesis of Cry2Aa in *B. thuringiensis* subsp. *kurstaki* [15]. The role (if any) of Orf1 and P19 in crystallization of Cry in *B. thuringiensis* or in *E. coli* is not known yet.

In this study, *p19* was cloned and its product characterized. The correct sequence was confirmed by comparing all available isolates of *B. thuringiensis* subsp. *israelensis*. Each of the genes, *p20* and *p19*, was cloned in *E. coli* together with *cyt1Aa* to investigate their possible interactions. The effect of GroEL and GroES chaperones on Cyt1Aa was also compared. Of the four, only P20 protected *E. coli* cells from the lethal effect of Cyt1Aa.

Materials and Methods

Bacterial strains and plasmid vectors. The following plasmids were hosted in *E. coli* strain XL-Blue MRF′ (Stratagene): PT7blue-2 (Novagen); pTG10 carrying *groES* and *groEL* [21; kindly provided by Pierre Golobinoff]; pUC9 with 9.7 kb *Hin*dIII fragment [19] of pBtoxis from *B. thuringiensis* subsp. *israelensis* [8]; pUHE-24S, a modified pUHE-24 from which one *Nco*I site was removed, leaving a unique *Nco*I site in the translation start codon. pUHE-24 is a descendant of pDS [18] containing T5 ribosome-binding-site (RBS) [11], two tandem *lacO* and the early T7 promoter P_{A1} (utilizing the usual *E. coli* RNA polymerase).

The following strains of *B. thuringiensis* subsp. *israelensis* were used as sources for the *cry11Aa* operon. 4Q5, IPS78, IPS 70, HD 567 (ONR60A), and HD 500 (kindly supplied by D. R. Zeigler of the Bacillus Genetic Stock Center, Columbus, OH).

Recombinant DNA methods (34). DNA modifications were performed and restriction enzymes were used as recommended by the suppliers (mostly New England BioLabs and US Biochemical). Competent cells were prepared and plasmids were isolated by standard procedures. Transformants of *E. coli* strains XL-Blue MRF′ were selected on Luria-Bertani (LB) broth plates containing ampicillin (100 $\mu g\ ml^{-1}$). DNA was visualized with ethidium bromide on horizontal agarose slab gels (0.7%). If necessary, DNA fragments were purified from the gels by phenol extraction [37]. The DNA of pBtoxis was isolated as described previously [7].

Polymerase Chain Reaction (PCR). Amplification was carried out with high fidelity Vent DNA polymerase (New England BioLabs), which contains $3' \rightarrow 5'$ exonuclease activity, in a DNA thermal cycler (Hybaid Ltd., Middlesex Twll, England) for a 28-reaction cycle each. The 9.7 kb *Hin*dIII fragment [19] from pBtoxis, which includes *cyt1Aa*, *p19*, *cry11Aa*, and *p20*, was used as a template for all PCR reactions to amplify these genes.

The two primers employed to obtain the reported *p19* were: a 33-mer 5′-GGGAGAGAAGA**CCATGG**GGGAATATGAATTTTGA-3′ containing an *Nco*I restriction site (**bold-faced** nucleotides (nt) 12–17), an inserted triplet (**G**GG) of glycine (nt 17–19) for constructing the *Nco*I site after ATG, and additional 25 nt of the *p19* coding sequence; a 24-mer 5′-ATAGTGAAGTG**AAGCTT**TCCTTTA-3′ containing a *Hin*dIII restriction site (**bold-faced** nt 12–17) and 18 nt additional of the coding sequence. Reaction cycle parameters consisted of 1 min at 94°C, 1 min at 50°C and 40 s at 72°C.

The two primers employed to obtain the correct sequence of *p19* were: the same 33-mer as used above to obtain the original *p19*; a 32-mer 5′-CTAAAGAAC**AAGCTT**GCATATAATTCATTCCA-3′ containing a *Hin*dIII restriction site (**bold-faced** nt 10–15), and additional 26 nt of the *p19* coding sequence. Reaction cycle parameters employed were identical to those above.

The two primers employed to obtain *p20* were: a 30-mer 5′-GGAGGAT**CCATGG**GGACAGAAAATGGAGTG-3′ with the *Nco*I site at 8–13 nt, the inserted glycine triplet at 13–15 nt, and additional 22 nt of the *p20* coding sequence; a 21-mer 5′-CTTGA**AAGCTT**A-AACGTTCCG-3′ with the *Hin*dIII restriction site at 6–11 nt, and additional 15 nt of the coding sequence. Reaction cycle parameters consisted of 1 min at 94°C, 1 min at 47°C and 40 s at 72°C.

The two primers employed to obtain *cyt1Aa* were: a 26-mer 5′-GGCCACTATTCTAAT**AAGCTT**AAGGA-3′ containing a *Hin*dIII restriction site (**bold-faced** nucleotides (nt) 16–21), and additional 20 nt of the *cyt1Aa* coding sequence; a 23-mer 5′-GGGGAA**TCTA-GA**TTAACGCATGA-3′ containing an *Xba*I restriction site (**bold-faced** nt 7–12) and additional 17 nt of the coding sequence. Reaction cycle parameters consisted of 1 min at 94°C, 1 min at 60°C and 1 min at 72°C.

Construction of the plasmids. The blunt-end PCR products (525, 567, and 873 bp fragments for *p19*, *p20*, and *cyt1Aa*, respectively) were digested with *Nco*I/*Hin*dIII (*p19* and *p20*) or *Hin*dIII/*Xba*I (*cyt1Aa*) and inserted into the same sites of pUHE-24S to get pRM4-19, pRM4-R, and pRM4-C, respectively (Fig. 1). The two combinations with *cyt1Aa* were cloned as follows: *cyt1Aa* was removed from the MCS of pRM4-C by *Hin*dIII/*Xba*I and inserted into the same sites of pRM4-19 and pRM4-R, respectively, downstream from *p19* and *p20*, to yield clones pRM4-19C and pRM4-RC.

DNA sequences. The *p19* sequences were determined by two methods. (I) Manually, by the dideoxy chain-termination method [35] using the Thermosequenase radiolabelled Terminator Cycle Sequencing kit and [^{33}P]dNTPs (1500 Ci/mmole or 55.5 TBq/mmole; Amersham), following the standard protocol supplied by the manufacturer. Briefly, 45 μCi of each of four Redivue a [^{33}P] dideoxy nucleotide (G, A, T, C) terminators were used to radiolabel four different DNA sequencing reactions by the Thermosequenase™ DNA polymerase (Amersham). Initial denaturation and subsequent cycling conditions were performed as described in PCR with only one specific primer. The reaction products were then denatured by stop solution containing 95% formamide and heating at 70°C for 2–10 min. The products were then electrophoresed on DNA sequencing gels (6% acrylamide, 7 M urea and 1×TBE) at 50 W constant power for 4–8 h. Autoradiography was

carried out using Kodak BioMax MR films. In all cases, DNA sequences were confirmed by sequencing both DNA strands.

(II) Automatically, by ABI PRISM dye terminator cycle sequencing ready reaction kit with AmpliTaq DNA polymerase FS and DNA sequencer ABI model 373A system (Perkin-Elmer) using the following primers: from 5′ of the multiple constriction site (MCS), D-pUHE, CGAGGCCCTTTCGTCTTCACCTCG; from inside of *p19* 5′ direction, p19-D-inside GCTGTGAGTTGCCAAGATACTGTCTGCG; from 3′ direction of MCS, Tz-1 primer, CTGGATCTATCAACAGGAGTCCAAGC; from 3′ direction of *p19* CTAAAGAACTATCCCGGGTATAATTCATTCCA.

In vitro transcription-translation system. The coding DNA was cloned into PT7blue-2 that includes PT7 promoter with *Nco*I/*Hin*dIII. The recombinant plasmid was obtained by High pure plasmid isolation kit (Boehringer Mannheim) and further purified twice with chloroform/ethanol to insure that it is RNAse-free. Single tube protein system 3 (Novagen) was used for a single step efficient in vitro synthesis of proteins; transcription with T7 polymerase was directly followed by translation in an optimized rabbit reticulocyte lysate. Plasmid DNA (0.5 μg) was added to 8 μl of transcription mix and transcribed at 30°C for 15 min, followed by addition of 40 μl translation mix and continued incubation for 90 min. The product was analyzed on SDS polyacrylamide gel.

Gene expression. Transgenic *E. coli* cells were grown at 37°C in LB broth supplemented with 100 μg ml^{-1} ampicillin and induced by isopropyl β-D thiogalactoside (IPTG; 0.5 mM) when the culture reached optical density of 0.2–0.3 (Ca. 2×10^8 cells ml^{-1}). Cells were harvested by centrifugation 4 h later, re-suspended in distilled water, and aliquots were boiled (10 min) in sample treatment buffer (62.5 mM Tris-Cl, 2% SDS, 10% glycerol, 0.01% Bromophenol blue and 0.1 M DTT). Protein profiles analyzed by discontinuous sodium dodecyl sulfate polyacrylamide gel electrophoresis (SDS-PAGE) using 4.5% and 12% acrylamide (pH 6.8 and 8.8) as the stacking and separating gels, respectively [28]. For gels with 6 M urea, 5% stacking and 15% separating acrylamide was employed. In addition, pre-cast Tris-Glycine 10–20% wide range gel (Novex) was used. When DTT concentration was modified, it was stated in the figure legend. Protease inhibitor AEBSF Hydrochloride was added at 4 mM (final concentration) during sample preparations to prevent proteolysis. The gels were stained with 0.1% Coomassie blue R-250. Protein concentrations were measured [10] with bovine serum albumin as the standard, and an equal amount of total protein was loaded on each slot.

To block sulfhydril groups, they were alkylated [42]. Samples were boiled in treatment buffer with higher ionic strength (0.4 mol/L) at pH 8.0, and 10 μl of iodoacetamide solution (20%) was added per 100 μl and incubated in dark for 30 min at room temperature.

Western Blot. Proteins were electrotransferred from SDS polyacrylamide gel onto nitrocellulose membranes and exposed to specific antiserum directed against Cyt1Aa (kindly provided by Sarjeet Gill, University of California, Riverside) or P20 (kindly provided by David Ellar, University of Cambridge). Protein A-alkaline phosphatase conjugate was used as a primary antibody detector. Visualization of the antigen was done with sigma fast-5-bromo-4-chloro-3-indolylphosphate/nitro blue tetrazolium tablets (Sigma Chemical Co), the chromogenic substrate for alkaline phosphatase.

Necleotide sequence accession number. The full nucleotide sequence of the correct *p19* is available in EMBL and GenBank nucleotide sequence databases under accession number AJ010753.

Results

Expressing *p19* in *E. coli*. The putative 19-kDa polypeptide encoded by the open reading frame *p19* in the *cry11Aa* operon [17] may be involved in crystallization of Cyt1Aa similarly to P20 [2]. To find out whether it protects *E. coli* cells from the lethal action of Cyt1Aa [19], *p19* was amplified with appropriate primers according to the published sequence [17] and cloned, alone or in combination with *cyt1Aa*. A parallel set of combinations was cloned as well, of *cyt1Aa*, *p20*, and both of them together (see Materials and Methods and Fig. 1).

Recombinant *E. coli* carrying pRM4-19 was grown and induced with IPTG for 4 h and the protein content analyzed on SDS polyacrylamide gel (Fig. 2). An additional polypeptide was detected, but its electrophoretic mobility corresponded to molecular mass significantly higher than the expected 19 kDa. The discrepancy in size led us to sequence the encoding cloned gene. The published sequence [17] predicts a polypeptide shorter by nine amino acids due to an additional C, shifting the open reading frame to yield an ochre codon (TAA) after the 170th amino acid. The additional C shifted the reading frame from the 168th codon (Fig. 3). The predicted molecular weight of the correct polypeptide containing 179 amino acids is 19,972 Da.

The sequence obtained by us did not derive of a mutation in the template nor during PCR amplification. The same C was missing in the gene repeatedly isolated and sequenced from pBtoxis [8] of 5 different isolates of *B. thuringiensis* subsp. *israelensis*, 4Q5, IPS78, IPS70, HD500, and HD567 (the latter was the source of the published gene). The same sequence was obtained by the two methods employed, and from both strands, and introduced into EMBL and GenBank nucleotide sequence database (Accession number AJ010753).

Expressing the correct *p19*. Another 3′ primer, designed according the new sequence (Fig. 3B), was used to amplify *p19*. The new gene was cloned as before to yield pRM4-19N (Fig. 1), and its expression was induced similarly. The mobility obtained with SDS-PAGE was also significantly slower than expected (Fig. 4, lane 5). This could be affected by the high-cysteine content (11.1%) in P19. To allow full reduction of the many possible disulfide bonds, higher concentrations of DTT (0.3–2 M) were used without a significant change in mobility pattern (Fig. 4, lanes 1–4). A systematic reduction of P19 abundance and simultaneous formation of high molecular weight proteins near the slots with increased DTT concentration (Fig. 4, lanes 1–3) are obvious.

To eliminate the possibility that the unexpected size of P19 is connected with expression in the host cell, an in

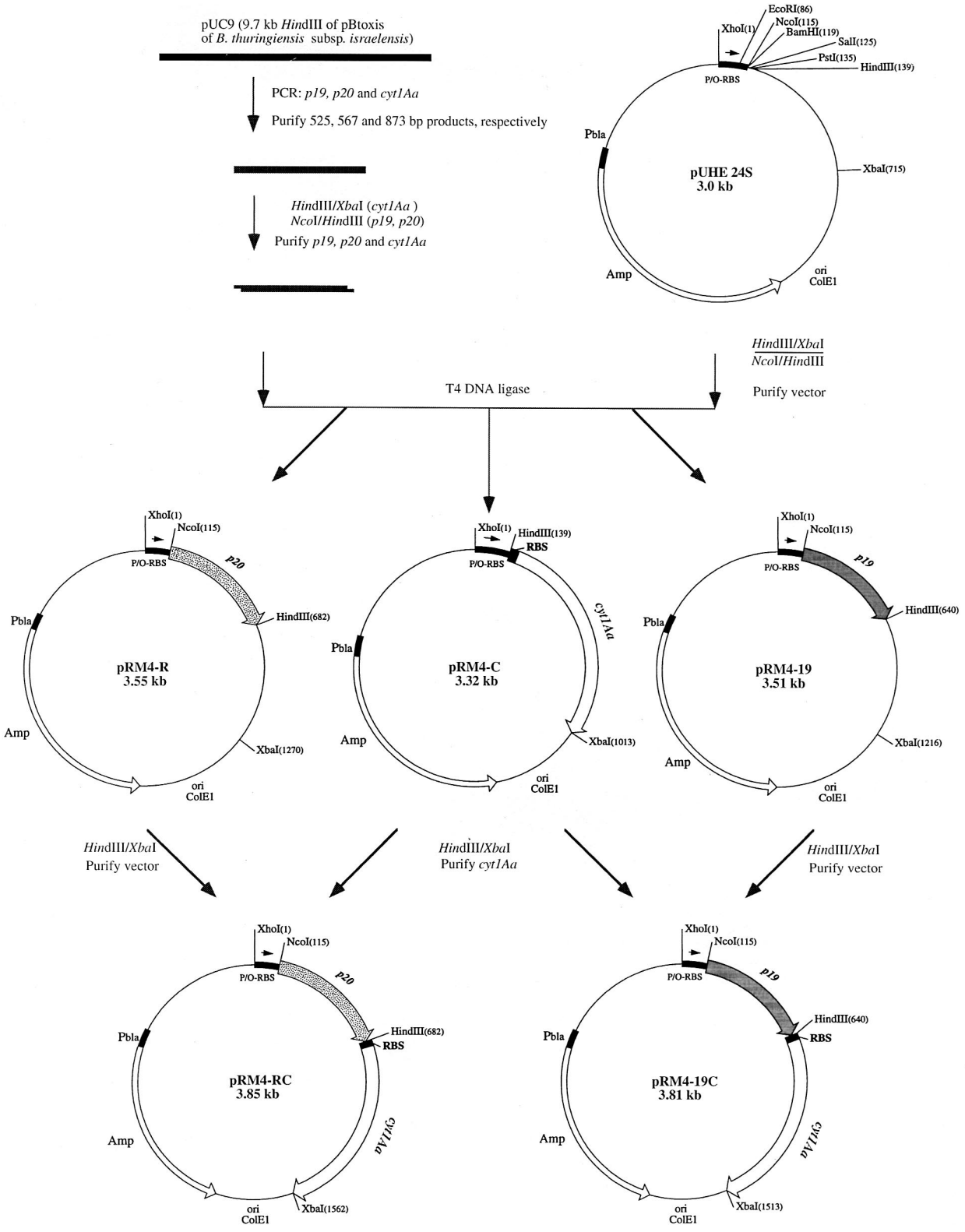

Fig. 1. Construction of expression vectors pRM4-19, pRM4-R, pRM4-C, pRM4-19C, and pRM4-RC (as described in Results).

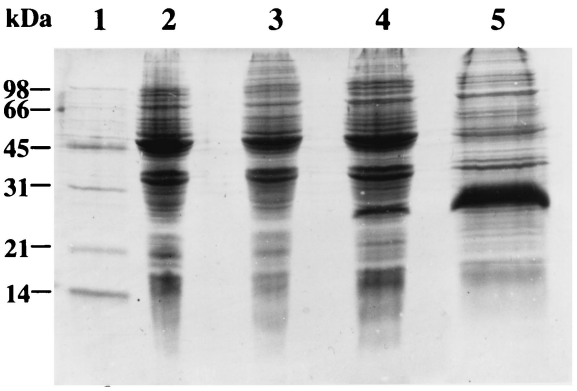

Fig. 2. SDS PAGE analysis of *p19* gene expression in *E. coli*. Lane **1**, molecular size marker. Extract of the clone harboring pUHE-24S, without (lane **2**) or after 4 h induction (lane **3**). Extract of the clone harboring pRM4-19, without (lane **4**) or after 4 h induction (lane **5**).

vitro transcription-translation system was employed. In this system, the only gene translated, *p19* in this case, is the one cloned into PT7blue-2 controlled by T7 promoter. The resultant polypeptide had again the same size as that expressed in *E. coli* (Fig. 5, lane 2). The slower migration of P19 in SDS-PAGE thus seems to derive from its unusual intrinsic structure.

The well-detectable band of P19 (Fig. 6A, lane 3) disappeared on the same gel in unreduced conditions (lane 5). In this last case, which was a pre-cast Tris-glycine 10–20% wide range gradient gel, another phenomenon was observed: P19 was now detected above the 31 kDa marker and not below it as in previous gels (Figs. 2, 4, 5). Would urea complete the unfolding of P19 on SDS gel? In the presence of 6 M urea (Fig. 6B), P19 displayed a similar apparent molecular weight, and disappeared in the absence of DTT (compare lanes 3 and 4 with lane 5), as it did without urea. A similar effect to that observed under unreduced conditions was obtained when samples boiled under reduced conditions were further treated with iodoacetamide (Fig. 6C); the sulfhydryl groups were thus apparently better protected by alkylation.

Combinations of *p19, p20,* and *cyt1Aa,* and interactions between their products. After addition of the gratuitous inducer IPTG to an LB culture of the clone with pRM4-C, the turbidity stopped increasing (Fig. 7A), culminating in reduced viable counts by four orders of magnitude (data not shown), as previously found [19]. Cells of *E. coli* expressing both *cyt1Aa* and *p20* (harboring pRM4-RC) continued to grow at the same rate as before induction (Fig. 7B), demonstrating that P20 protects them from the lethal effect of Cyt1Aa, as has been demonstrated in *B. thuringiensis* subsp. *kurstaki* (cryB) [45]. On the other hand, P19 failed to protect the host cells from the lethal action of Cyt1Aa: the clone with pRM4-19C, expressing both *p19* and *cyt1Aa*, behaved similarly to the one with pRM4-C, expressing *cyt1Aa* alone (Fig. 7C).

Western blot analysis was performed for all clones with polyclonal anti-Cyt1Aa (Fig. 8). The amount of Cyt1Aa was higher when expressed together with P20, and lowest with P19 (compare lane 1 with 2, and lane 5 with 6). Expression of P20 was similarly demonstrated by polyclonal anti-P20 in strains carrying pRM4-R and pRM4-RC (data not shown).

Effects of Gro-EL and Gro-ES on Cyt1Aa. P20 is required to produce large amounts of Cyt1Aa in *E. coli* [1, 32, 40] and is not required in strains carrying mutations in *rpoH, groEL,* or *dnaK* [40], all of which reduce the proteolytic ability of the cells [4]. To find out whether this activity of P20 is chaperone-like, the effects of GroEL and GroES on the level of Cyt1Aa and on killing the host were tested. *E. coli* carrying pRM4-C was transformed by pTG10 over-expressing *groES* and *groEL* [21]. Excess GroESL did not prevent the lethal effect of Cyt1Aa (Fig. 7D), neither did it affect dramatically the amount of Cyt1Aa (Fig. 8), as might have been expected from previous results [40].

Discussion

Structure of the enigmatic *P19*. Expression of *p19* alone (from pRM4-19) resulted in a polypeptide (Fig. 2) with an estimated size (by SDS-PAGE) significantly higher than predicted by its known sequence [17]. Sequencing of our cloned *p19* discovered a cause for the discrepancy. The gene from five different isolates of *B. thuringiensis* subsp. *israelensis*, 4Q5, IPS78, IPS70, HD500, and HD567 (the latter was the source of the published gene; [17]), had a missing C (compared to the original sequence). The resulting polypeptide is longer by nine amino acids than the published one (Fig. 3). The same sequence was obtained by the two methods employed, and from both strands.

The correct sequence of *p19* predicts a protein product of 179 amino acids with a calculated molecular weight of 19,972 Da. Yet, it is made in *E. coli* as a 28 kDa polypeptide (based on SDS-PAGE mobility; Fig. 4), ca. 40% larger than predicted. A product with similar mobility was observed in vitro when *p19*-specific mRNA was translated in a cell-free system (Fig. 5), confirming that this feature is an intrinsic property of P19 not influenced by post-translational modification in *E. coli*. The aberrant mobility of P19 does not seem to result from some structural feature imposed by its high content

```
                                  *
A  GAT TGT GAT TGT CAC GCC GGT GAA AAT TAA
   asp cys asp cys his ala gly glu asn

   162 163 164 165 166 167 168 169 170 171 172 173 174 175 176 177 178 179

B  GAT TGT GAT TGT CAC GCG GTG AAA ATT AAA GGG AAA TTT TCA CTT CAC TAT AAA TAA
   asp cys asp cys his ala val lys ile lys gly lys phe ser leu his tyr lys
```

Fig. 3. Nucleotide (and derived amino acids) sequences. Comparison between the 3′-end (and C-terminus) of the original published [17] *p19* (**A**) and of the real *p19* **(B)**. Numbers represent the codons. The additional C is labeled by an asterisk.

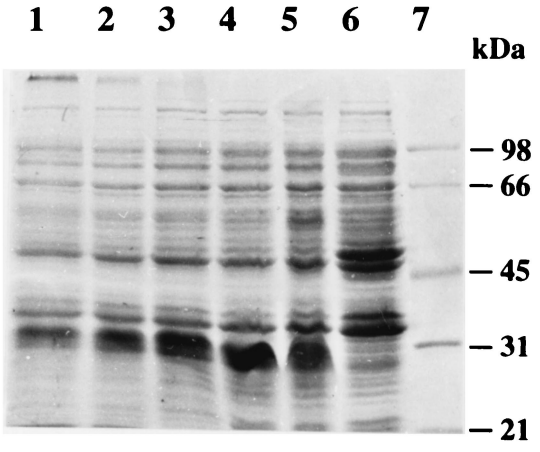

Fig. 4. SDS PAGE analysis of the correct P19 expressed in *E. coli*. Lane **6**, extract of the clone harboring pRM4-19N without induction. Lanes **1–5**, after 4 h induction, treated with different concentrations of DTT in sample buffer:(2, 1, 0.7, 0.3, and 0.1 M, respectively). Lane **7**, molecular size marker.

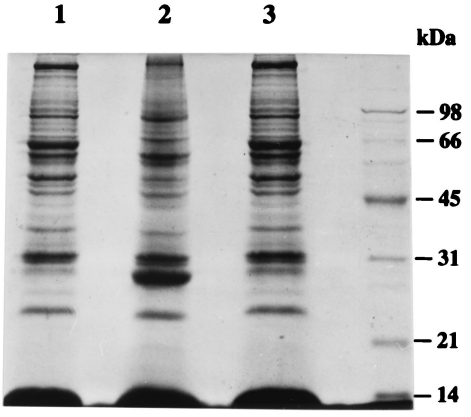

Fig. 5. SDS PAGE analysis of in vitro P19 synthesis. Protein expressed by Novagen's transcription-translation system 3. Lane **1**, PT7blue-2 alone; lane **2**, PT7blue-2 that includes *p19*; lane **3**, PT7blue-2 that includes *p19*, without sodium-acetate precipitation. Molecular size markers are indicated on the right.

(11.1%) of cysteines: no change in migration pattern was noted under high dithioerythritol (DTT) concentrations (Fig. 4, lanes 1–3). The additional high molecular weight band near the slots formed in excess of DTT is probably caused by aggregation of P19 with itself or other proteins (Fig. 4, lanes 1–3), as indicated by the lower abundance in the P19 and other bands.

Orf2 from *B. thuringiensis* subsp. *kurstaki* displays a similar anomaly: its electrophoretic mobility corresponds to a molecular mass of 50 kDa despite a predicted size of 29 kDa [43]. This phenomenon was also recorded in small spore-coat proteins of *B. subtilis* [47], and may thus shed light on the nature of P19 and its function.

Higher apparent molecular weight may be due to residual secondary structures retarding P19 migration on the gel. Addition of urea for better dissociation did not change its aberrant mobility above the 31 kDa marker (Fig. 6B), as obtained with the Tris-glycine gradient gel (Fig. 6A).

In the absence of DTT, P19 was no longer visible, whether running with urea or without (Fig. 6, B and A, respectively). This observation can be explained by the high number (20 out of a total of 179 amino acids) of cysteine residues as follows. Reduction of all disulfide bonds by DTT forms a single P19 band of at least 28 kDa (depending on the type of gel and running conditions). Unreduced P19, on the other hand, smears by running as multiple bands due to variation in disulfide bond conformations and SDS binding capacity (depending on accessibility to the amino groups), hence it would apparently disappear due to bands' dilution. Reformation of its disulfide bridges during migration on the gel, which was blocked by alkylation of the SH groups with iodoacetamide after reduction with DTT, caused its disappearance, as happens under unreduced conditions (Fig. 6C, compare lanes 2 and 3). The observed band of reduced P19 may thus represent a single major conformation of the re-oxidized polypeptide. We are currently involved in purifying P19 for further characterization, to extend the results obtained here.

P20 and P19 as potential accessory proteins. Crystal formation in *B. thuringiensis* prevents proteolytic degradation of the δ-endotoxin. The resultant protease-resistant crystalline body, which can account for up to 25% of the dry weight of the sporulating cell, involves a high

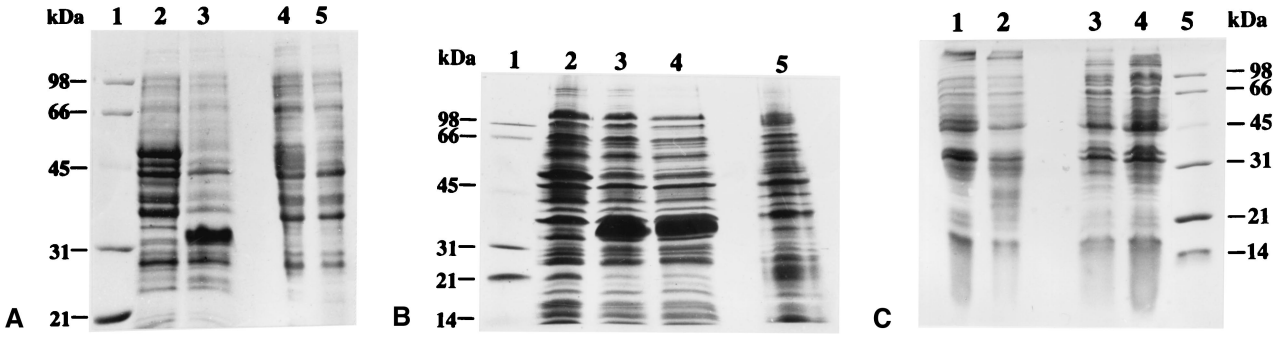

Fig. 6. SDS-PAGE analyses of P19 in extracts of the clone with pRM4-19N, under reduced and unreduced conditions, supplemented with urea or treated with iodoacetamide. (**A**) Cultures growing exponentially and after 4 h induction, either treated with 0.1 M DTT in the sample buffers (lanes **2** and **3**, respectively), or not (lanes **4** and **5**, respectively). Lane **1**, molecular size marker. (**B**) The SDS-PAGE was supplemented with 6 M urea. Cultures growing exponentially (lane **2**) and after 4 h induction (lanes **3–5**). The samples were treated with the following DTT concentrations: 0.5 M (lane **4**), 0.1 M (lanes **2** and **3**), or none (lane **5**). Lane **1**, molecular size marker. (**C**) Extracts of exponentially growing culture (lanes **1** and **4**) and after 4 h induction (lanes **2** and **3**), treated in the sample buffers with 0.2 M DTT and 4 mM iodoacetamide (lanes **1** and **2**), or not (lanes **3** and **4**). Lane **5**, molecular size marker.

number of toxic proteins expressed from strong promoters of the appropriate *cry* genes in the late stationary-phase [2, 5]. The C-termini of the largest ICPs seem to be involved in packaging the polypeptides within the crystalline inclusion [22]. Intermolecular disulfide bridges between cysteine residues within the C-terminal domains of Cry1 [9] support this hypothesis. The ability of smaller δ-endotoxins to form crystals despite lack of cysteine-rich C-termini indicates that other factors are involved in their crystallization. Indeed, for assembly of inclusion bodies, Cry2Aa requires the accessory protein Orf2 and both Cry11Aa and Cyt1Aa require P20 [1, 15, 20, 32, 40, 46]. Their respective genes are organized in strikingly similar operons: *cry2Aa* is co-transcribed with *orf1/orf2* and *cry11Aa* is co-transcribed with *p19/p20* [5, 17, 43].

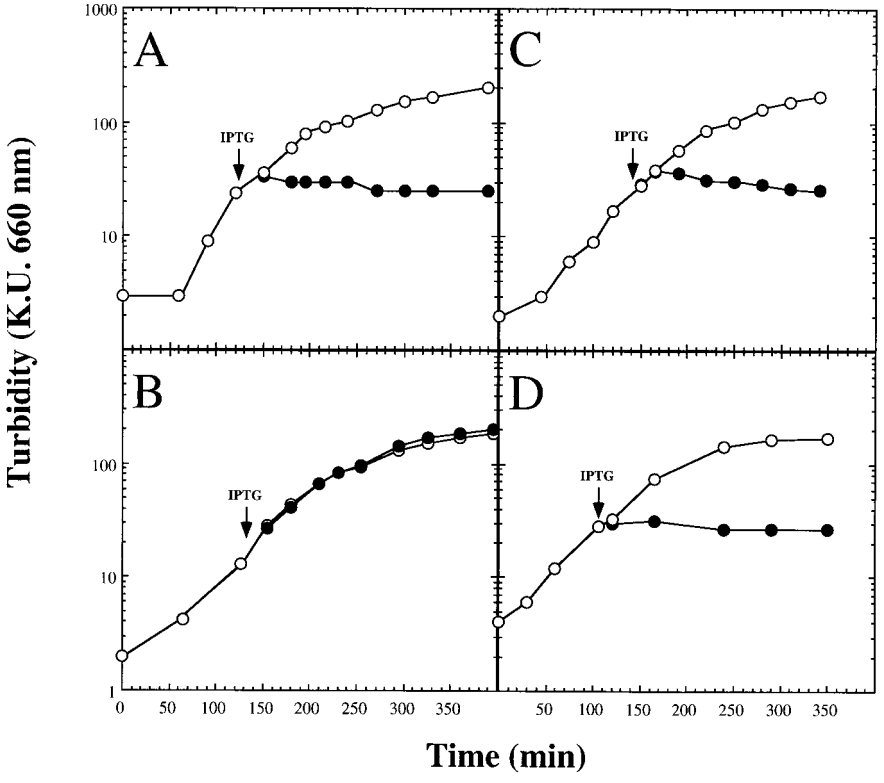

Fig. 7. Mass growth of exponentially growing *cyt1Aa*-containing *E. coli* (○) and after induction (●) with IPTG. Clones (Fig. 1) harboring pRM4-C (**A**), pRM4-RC (containing also *p20*) (**B**), pRM4-19C (containing also *p19*) (**C**), and pRM4-C plus pTG10 (containing *groELS*) (21) (**D**). IPTG was added (arrows) when the culture reached 25 K.U.

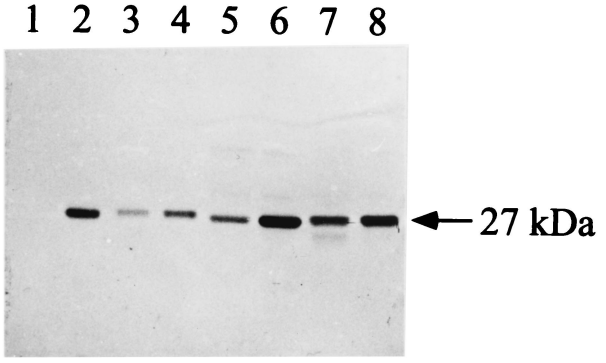

Fig. 8. Immunoblot of Cyt1Aa in extracts of cells expressing *cyt1Aa* (Fig. 7). Cells with pRM4-19C (lane **1**), pRM4-RC (lane **2**), with pRM4-C (lane **3**), and with pRM4-C plus pTG10 (lane **4**). Lanes **5–8**, the same as **1–4** but with fivefold higher extract concentrations.

cyt1Aa, on the other hand, is mono-cistronic but also coordinatively regulated with *cry11Aa* [1].

Early studies concluded that P20 was required for efficient Cyt1Aa production in *E. coli* [1, 32, 40], but its lethal effect on the recombinant host was not detected. The general cytotoxic effects of Cyt1Aa [22, 39] was later extended to *E. coli* [19, 41] and *B. thuringiensis* subsp. *kurstaki* [45]. The lethal effect was observed in our clones: the dramatic loss (4 orders of magnitude) of colony forming ability (data not shown, see [19]) was not associated with cell lysis (Fig. 7).

Mass-growth inhibition of recombinant *E. coli* soon after induction of *cyt1Aa* was not related to high level of the heterologous protein: cell viability was lost quicker than rate of protein accumulation (data not shown). Moreover, cells remained viable when Cyt1Aa concentration was higher in the P20-co-expressing strain (carrying pRM4-RC) (Fig. 8, lane 6).

We have previously proposed that P20 may protect recombinant *E. coli* from the lethal effect of Cyt1Aa [19], as it prevents proteolysis [1, 32, 40], by specific interactions between them. This prediction has been confirmed in an acrystalliferous strain of *B. thuringiensis* subsp. *kurstaki* [45], and is demonstrated here for the first time in *E. coli* (Fig. 7B) by expressing both proteins in the same cell (carrying pRM4-RC; Fig. 1) from the inducible P_{A1} promoter. When produced together, P20 indeed stabilized Cyt1Aa (Fig. 8) and prevented growth inhibition (Fig. 7B) and cell death (data not shown) by this cytotoxic protein. These dramatic effects may be associated with modified Cyt1Aa function rather than level of expression (Fig. 8, compare lane 2 with 4, and lane 6 with 8).

The mechanism(s) by which P20 and Orf2 exert their effects on crystal formation is(are) not well understood. It is generally claimed that P20 allows crystallization of several δ-endotoxins. Expression of *cyt1Aa* in acrystalliferous strains of *B. thuringiensis* resulted in large ovoidal, lemon-shaped inclusions only when *p20* was co-expressed from a very strong promoter [13, 16, 45]. There is, however, more evidence that P20 allows high yields and accumulation of crystal proteins rather than takes a direct role in the crystallization process itself. For example, more Cry11Aa was produced in recombinant *E. coli* carrying *p20* than in those without it [40]. Induction of *cry11Aa* in *E. coli* yields larvicidal activity only when produced together with P20 [6]. Expression of *p20* in tandem with truncated *cry1C* in acrystalliferous *B. thuringiensis* subsp. *kurstaki* led to production of greater amount of Cry1C without appearance of inclusion bodies [33]. Likewise, inclusions of Cry4Aa were not formed in acrystalliferous *B. thuringiensis* subsp. *israelensis* even when *p20* was co-expressed [16]. The yield of Cry2Aa in *B. thuringiensis* subsp. *israelensis* was indeed higher in the presence of either P20 or Orf2, and highest with both [20], but typical Cry2Aa crystals were formed only in constructs including *orf2* [20]. Disruption of *orf2* led to reduction of Cry2Aa and total lack of its crystals [15], or to aggregation of a distinct lattice [20]. Involvement of Orf2 in Cry2Aa crystallization seems to be due to its unique structure, with 11 tandem repeats of a 15-amino acids sequence [43]. This structure may provide the matrix, template, or scaffold for crystallization [20].

All these observations support the view that P20 allows accumulation of toxic proteins but not crystallization. Among others, nascent Cyt1Aa is protected from proteolysis before maturation [1, 40]. This hypothesis is supported by the observation that *E. coli* strains (carrying mutations in *rpoH*, *groEL*, or *dnaK*) with reduced ability to degrade abnormal proteins produce the same amount of Cyt1Aa without P20 as they do with P20 [40]. It is not clear why *E. coli* identifies Cyt1Aa as an abnormal protein targeted for degradation by the heat shock proteins. In addition to protein folding function, the molecular chaperones GroEL and GroES are required for rapid degradation of certain abnormal proteins in *E. coli*, particularly heterologous [23]. On the other hand, high levels of GroEL and GroES, well-established chaperones [31, 38], did not stabilize Cyt1Aa as P20 did (Fig. 8, compare lane 3 with 4, and lane 7 with 8) nor did it prevent the lethal effect of Cyt1Aa (Fig. 7B, D; viability data not shown).

The lethal effect of Cyt1Aa in *E. coli* may be due to its activation by incomplete degradation by this system. According to this view, P20 protects Cyt1Aa from such degradation thus prevents its lethal effect. This is confirmed by the observed co-immuno-precipitation of P20 and Cyt1Aa in extracts of *E. coli* expressing both [40].

Cyt1Aa-P20 complex would then be a poor substrate for proteolysis, or P20 would block a protease-susceptible site of Cyt1Aa by binding to it. Alternatively, P20 may help the mature protein to form a dimer [14], which is the stable native pro-toxin, similarly to that found for Cyt2Aa [30]. Whatever the mechanism is, P20 is considered to protect Cyt1Aa from unspecific full proteolysis as well as from cleavage in specific site that activates it to kill *E. coli*.

Hence, the role of P20 in ICP production is questionable as a chaperone. It is not necessary for crystallization of Cyt2Aa in *E. coli*, as Orf2 is not for Cry2Ac crystallization in *B. thuringiensis* subsp. *kurstaki* [2, 44]. Their roles may not be of general nature and their designation as helper proteins [2, 26] may be more appropriate.

Being expressed coordinately with Cry11Aa and P20 from the same promoter, P19 has been considered to have some role in their crystallization, particularly when that of P20 became less clear [2]. It may thus also protect host recombinant cells from the lethal action of Cyt1Aa, as does P20. This idea was precluded here: when the respective genes were co-expressed, the real P19 (Fig. 3) did not protect *E. coli* (Fig. 7C, and data not shown), neither did it stabilize Cyt1Aa (Fig. 8), as did P20. The amount of Cyt1Aa obtained in the clone (pRM4-19C) with the genes for both was lower even than in the clones without *p19*, whether alone or with *groELS* (Fig. 8). Whether it can protect *B. thuringiensis* subsp. *kurstaki* from the lethal action of Cyt1Aa [45] is still to be determined.

Its function remains enigmatic, as does the function of the highly similar (33% identity) Orf1 [17]. It is even more intriguing since *orf1* homologues have also been identified as members of the *cry2Ac* and *cry9Ca* operons [29, 44].

ACKNOWLEDGMENTS

This investigation was partially supported by a grant (No. 801-8) from the Israel Ministry of Environment, a grant (No. 97-00081) from the United States–Israel Binational Science Foundation (BSF), Jerusalem, Israel (A.Z.), and a post-doctoral fellowship (E.B.-D.) from the Israel Ministry of Science. Thanks are due to D.R. Zeigler for *Bti* strains, to S. Leu and P. Golobinoff for pUHE-24S and pTG10, respectively, to S.S. Gill and D.J. Ellar for antisera against Cyt1Aa and P20, respectively, and to G. Raziel for photography. C. Aflalo and J. Eichler are gratefully acknowledged for constructive advice regarding protein structure analysis.

Literature Cited

1. Adams LF, Visick JE, Whiteley HR (1989) A 20-kilodalton protein is required for efficient production of the *Bacillus thuringiensis* subsp. *israelensis* 27-kilodalton crystal protein in *Escherichia coli*. J Bacteriol 171:521–530
2. Agaisse H, Lereclus D (1995) How does *Bacillus thuringiensis* produce so much insecticidal crystal protein? J Bacteriol 177: 6027–6032
3. Aronson AI (1993) The two faces of *Bacillus thuringiensis* insecticidal proteins and post-exponential survival. Mol Microbiol 7:489–496
4. Baker TA, Grossman AD, Gross CA (1984) A gene regulating the heat shock response in *E. coli* also causes a defect in proteolysis. Proc Natl Acad Sci USA 81:6779–6783
5. Baum JA, Malvar T (1995) Regulation of insecticidal crystal protein production in *Bacillus thuringiensis*. Mol Microbiol 18: 1–12
6. Ben-Dov E, Boussiba S, Zaritsky A (1995) Mosquito larvicidal activity of *Escherichia coli* with combinations of genes from *Bacillus thuringiensis* subsp. *israelensis*. J Bacteriol 177:2851–2857
7. Ben-Dov E, Einav M, Peleg N, Boussiba S, Zaritsky A (1996) Restriction map of the 125-kilobase of *Bacillus thuringiensis* subsp. *israelensis* carrying the genes that encode delta-endotoxins active against mosquito larvae. Appl Environ Microbiol 62:3140–3145
8. Ben-Dov E, Nissan G, Peleg N, Manasherob R, Boussiba S, Zaritsky A (1999) Refined, circular restriction map of the plasmid of *Bacillus thuringiensis* subsp. *israelensis* carrying the mosquito larvicidal genes. Plasmid 42:186–191
9. Bietlot HPL, Vishnubhatla I, Carey PR, Pozsgay M, Kaplan H (1990) Characterization of the cysteine residues and disulfide linkages in the protein crystal of *Bacillus thuringiensis*. Biochem J 267:309–315
10. Bradford MM (1976) A rapid and sensitive method for the quantitation of microgram quantities of protein utilizing the principle of protein-dye binding. Anal Biochem 72:248–254
11. Bujard H, Gentz R, Lanzer M, Stueber D, Mueller M, Ibrahimi I, Haeuptle MT, Dobberstein B (1987) T5 promoter-based transcription-translation system for the analysis of proteins *in vitro* and *in vivo*. Methods Enzymol 155:416–433
12. Chang C, Dai SM, Frutos R, Federici BA, Gill SS (1992) Properties of 72-kilodalton mosquitocidal protein from *Bacillus thuringiensis* subsp. *morrisoni* PG-14 expressed in *B. thuringiensis* subsp. *kurstaki* by using the shuttle vector pHT3101. Appl Environ Microbiol 58:507–512
13. Chang C, Yu YM, Dai SM, Law SK, Gill SS (1993) High-level *Cry11A* and *cytA* gene expression in *Bacillus thuringiensis* does not require the 20-kilodalton protein, and the coexpressed gene products are synergistic in their toxicity to mosquitoes. Appl Environ Microbiol 59:815–821
14. Couche GA, Pfannenstiel MA, Nickerson KW (1987) Structural disulfide bonds in the *Bacillus thuringiensis* subsp. *israelensis* protein crystal. J Bacteriol 169:3281–3288
15. Crickmore N, Ellar DJ (1992) Involvement of a possible chaperonin in the efficient expression of a cloned CryII δ-endotoxin gene in *Bacillus thuringiensis*. Mol Microbiol 6:1533–1537
16. Crickmore N, Bone EJ, Williams JA, Ellar DJ (1995) Contribution of the individual components of the δ-endotoxin crystal to the mosquitocidal activity of *Bacillus thuringiensis* subsp. *israelensis*. FEMS Microbiol Letts 131:249–254
17. Dervyn E, Poncet S, Klier A, Rapoport G (1995) Transcriptional regulation of the *cryIVD* gene operon from *Bacillus thuringiensis* subsp. *israelensis*. J Bacteriol 177:2283–2291
18. Deuschle U, Kammerer W, Gentz R, Bujard H (1986) Promoters of *Escherichia coli*: a hierarchy of *in vivo* strength indicates alternate structures. EMBO J 5:2987–2994
19. Douek J, Einav M, Zaritsky A (1992) Sensitivity to plating of

Escherichia coli cells expressing the *cytA* gene from *Bacillus thuringiensis* var. *israelensis*. Molec Gen Genet 232:162–165
20. Ge B, Bideshi D, Moar WJ, Federici BA (1998) Differential effects of helper proteins encoded by *cry2A* and *cry11A* operons on the formation of Cry2A crystals in *Bacillus thuringiensis*. FEMS Microbiol Letts 165:35–41
21. Goloubinoff P, Gatenby AA, Lorimer GH (1989) GroE heat-shock proteins promote assembly of foreign prokaryotic ribulose bisphosphate carboxylase oligomers in *Escherichia coli*. Nature 337:44–47
22. Hofte H, Whiteley HR (1989) Insecticidal crystal proteins of *Bacillus thuringiensis*. Microbiol Rev 53:242–255
23. Kandror O, Busconi L, Sherman M, Goldberg AL (1994) Rapid degradation of an abnormal protein in *Escherichia coli* involves the chaperones GroEL and GroES. J Biol Chem 269:23575–23582
24. Knowles B, Ellar DJ (1987) Colloid-osmotic lysis is a general feature of the mechanism of action of *Bacillus thuringiensis* δ-endotoxins with different insect specificities. Biochim Biophys Acta 924:509–518
25. Knowles BH, Blatt MR, Tester M, Horsnell JM, Carroll J, Menestrina G, Ellar DJ (1989) A cytolytic δ-endotoxin from *Bacillus thuringiensis* var. *israelensis* forms cation-selective channels in planar lipid bilayers. FEBS Lett 244:259–262
26. Koni PA, Ellar DJ (1993) Cloning and characterization of a novel *Bacillus thuringiensis* cytolytic delta-endotoxin. J Mol Biol 229: 319–327
27. Kumar PA, Sharma RP, Malik VS (1996) The insecticidal proteins of *Bacillus thuringiensis*. Adv Appl Microbiol 42:1–43
28. Laemmli UK (1970) Cleavage of structural proteins during the assembly of the head of bacteriophage T4. Nature 277:680–685
29. Lambert B, Buysse L, Decock C, Jansens S, Piens C, Saey B, Seurinck J, Van Audenhove K, Van Rie J, Van Vliet A, Peferoen M (1996) A *Bacillus thuringiensis* insecticidal crystal protein with a high activity against members of the family Noctuidae. Appl Environ Microbiol 62:80–86
30. Li J, Koni PA, Ellar DJ (1996) Structure of the mosquitocidal δ-endotoxin CytB from *Bacillus thuringiensis* subsp. *kyushuensis* and implications for membrane pore formation. J Mol Biol 257: 129–152
31. Martin J (1998) Protein folding assisted by the GroEL/GroES chaperonin system. Biochim 63:374–381
32. McLean KM, Whiteley HR (1987) Exspression in *Escherichia coli* of a cloned crystal protein gene of *Bacillus thuringiensis* subsp. *israelensis*. J Bacteriol 169:1017–1023
33. Rang C, Bes M, Lullien-Pellerin V, Wu D, Federici B, Frutos R (1996) Influence of the 20-kDa protein from *Bacillus thuringiensis* subsp. *israelensis* on the rate of production of truncated Cry1C proteins. FEMS Microbiol Letts 141:261–264
34. Sambrook J, Fritsch EF, Maniatis T (1989) Molecular Cloning: a Laboratory Manual, 2nd edition. Cold Spring Harbor, NY: Cold Spring Harbor Laboratory Press
35. Sanger F, Nicklen S, Coulson AR (1977) DNA sequencing with chain-terminating inhibitors. Proc Natl Acad Sci USA 74:5463–5467
36. Schnepf E, Crickmore N, Van Rie J, Lereclus D, Baum J, Feitelson J, Zeigler DR, Dean DH (1998) *Bacillus thuringiensis* and its pesticidal crystal proteins. Microbiol Molec Biol Rev 62:775–806
37. Seth A (1984) A new method for linker ligation. Gene Anal Techn 1:99–103
38. Sigler PB, Xu Z, Rye HS, Burston SG, Fenton WA, Horwich AL (1998) Structure and function in GroEL-mediated protein folding. Annu Rev Biochem 67:581–608
39. Thomas WE, Ellar DJ (1983) *Bacillus thuringiensis* var. *israelensis* crystal δ-endotoxin: effects on insect and mammalian cells *in vitro* and *in vivo*. J Cell Sci 60:181–197
40. Visick JE, Whiteley HR (1991) Effect of a 20-kilodalton protein from *Bacillus thuringiensis* subsp. *israelensis* on production of the CytA protein by *Escherichia coli*. J Bacteriol 173:1748–1756
41. Ward ES, Ellar DJ (1986) *Bacillus thuringiensis* var. *israelensis* δ-endotoxin. Nucleotide sequence and characterization of the transcripts in *Bacillus thuringiensis* and *Escherichia coli*. J. Mol. Biol. 191:1–11
42. Westermeier R (1993) Electrophoresis in practice. A guide to theory and practice. New York, NY: VCH Press
43. Widner WR, Whiteley HR (1989) Two highly related insecticidal crystal proteins of *Bacillus thuringiensis* subsp. *kurstaki* possess different host range specificities. J Bacteriol 171:965–974
44. Wu D, Cao XL, Bai YY, Aronson AJ (1991) Sequence of an operon containing a novel δ-endotoxin gene from *Bacillus thuringiensis*. FEMS Microbiol Letts 81:31–36
45. Wu D, Federici BA (1993) A 20-kilodalton protein preserves cell viability and promotes CytA crystal formation during sporulation in *Bacillus thuringiensis*. J Bacteriol 175:5276–5280
46. Wu D, Federici BA (1995) Improved production of the insecticidal CryIVD protein in *Bacillus thuringiensis* using *cryIA(c)* promoters to express the gene for an associated 20-kDa protein. Appl Microbiol Biotechnol 45:697–702
47. Zhang J, Fitz-James PC, Aronson A (1993) Cloning and characterization of a cluster of genes encoding polypeptides present in the insoluble fraction of the spore coat of *Bacillus subtilis*. J Bacteriol 175:3757–3766